Structures of Two-dimensional Ring Polymer Solutions using Bond Fluctuation Model

Donghan Shin, Eunsang Lee, and YounJoon Jung*

Department of Chemistry, Seoul National University, Seoul 08826, Korea
Received Date; Accepted Date (to be inserted by the publisher after your manuscript is accepted)

Abstract: This study attempts to reveal structures of two-dimensional ring polymer solutions in various polymer concentrations ranging from dilute to concentrated regime. Polymer sizes, single molecule structure factors, bond correlation functions and monomer density distribution functions from center of mass are given in order to clarify the polymer structures. Our study shows that a ring in dilute solution maintain pseudo-circular structure with self-avoiding walk (SAW) statistics, and it seems to be composed of two connecting SAW linear chains. In semidilute solutions, ring polymers are not entangled with each other and adopt collapsed configurations. Such assumption of collapsed structures in the semidilute regime gives an overlap concentration of $\varphi^* \sim N^{-1/2}$ where N is degree of polymerization. By normalizing the polymer concentration by these overlap concentration, we find universal behaviors of polymer sizes and structure factors regardless of N.

Keywords : Bond Fluctuation Model, ring polymer, two-dimensional polymer, overlap concentration

Introduction

Dimensional dependence of polymer structure and dynamics has attracted great attention from polymer chemists and physicist since most of biological macromolecules function in confined geometries.[1-3] Explaining behaviors of adsorbed polymers on the flat surface in laboratories and industries also requires knowledge for polymer physics in reduced dimension. Decreasing space dimension, conformational space of polymers is restricted, and novel properties not observed in real dimension emerge.[4,5]

One interesting example is structural difference between two- and three-dimensional (2D and 3D) linear polymers in melt phase. It is completely understood that concentrated long linear polymers in 3D are entangled to each other, so that monomer excluded volume are screened out which behave like an ideal chain.[6-9] Structures of 2D linear polymers have been intensively under investigated and those are shown to be somewhat different from 3D polymers, such that relatively small fraction of inter-penetration is observed. In dilute condition, a polymer follows self-avoiding walk (SAW) characterized by ν=3/4 in 2D (physics behind this will be discussed in the next section).[10-12] With increasing density, it starts to overlap with other polymers and gives ν=1/2. Even though Flory exponents of an ideal chain and the collapsed globule in 2D are both ν=1/2, a pair correlation function gives an insight to be considered for 2D linear polymers as segregated ones.[11]

Not only the reduced dimension but intrinsic topological constraints of a polymer restrict the conformational space. A ring polymer without chain end is one such example with topological interactions. Due to the bond noncrossability, concatenated and knotted configurations are completely forbidden.[13,14] There exist many molecules with circular morphology in nature especially in living organisms such as circular plasmids and circular DNAs. It is not sufficient to understand and to predict behaviors of such circular molecules only with the knowledge for linear polymers. In this context, structural and dynamical behaviors of rings have been intensively studied by theories,[13,15,16] experiments,[17,18] and simulations.[19-21] Recent works have revealed that a ring in asymptotic regime adopts segregated structure with a very small Flory exponent (ν=1/3) and shows slow dynamics which is decoupled to its small viscosity.[22] However, all above works are focused on 3D environment. As mentioned, most of macromolecules in nature are subject to the confined geometries, and observing equipment in laboratories such as an atomic force microscopy usually dealt with the objects adsorbed on the surface which are quasi two-dimensional.[8,23] A few number of works have investigated physical properties

of 2D rings,[24-26] one of which for the dilute ring polymer solution made an effort to elucidate that the ring structure depends on the intrinsic number of solvents inside the ring.[26] Since the connectivity of a 2D ring completely prevents the other molecules penetrating into and out of the ring, it is expected that such restriction makes the concentrated ring behave differently with linear counterpart. However, density dependence of 2D ring polymer properties is still open question, thus it is very worthwhile to study structures of 2D rings with increasing density from dilute to concentrated regime in order to address above questions.

In this article, we provide structural properties of 2D ring polymers in athermal condition using bond-fluctuation model (BFM) and Monte Carlo simulations.[27] BFM is very a simple but powerful model to reproduce polymer properties especially in the reduced dimension. With increasing density from dilute to concentrated regime, the effect of molecular overlap to the structure is discussed. The rest of this article is organized as follows. We first provide theoretical background for polymer physics in 2D, and explain BFM we used in this work. In results and discussion session, we show the size of polymers, bond correlation functions, single molecule structure factors, monomer's density distribution functions to provide a physical insight for the 2D ring polymer structures. Concluding remark follows in the final section.

Computational Method

We use Bond Fluctuation Model (BFM) first proposed by Cremasin[27] which is very efficient to observe and to identify polymer structures with relatively short computing time. Thus, we simulate simple polymers which obey following rules using BFM.

BFM is a model considering simple and coarse-grained monomers on the square lattice. These BFM polymers continuously try Monte Carlo sweeps according to the rules under satisfaction of SAW, in order to reach an equilibrium state. At this moment, transitions of configuration do not depend on energy or temperature, so we say this system is in the athermal system with an infinite temperature and is purely controlled by entropy.

At first, each monomer of a polymer occupies whole of a 1×1 lattice room as Figure 1(a) and each polymer is a group of monomers whose center is connected to others as shown in Figure 1(b). The state of which some monomers are sharing vertexes of rooms is forbidden as shown in Figure 1(c). In other words, each bond can not be shorter than 2(=√4) which mimics the positive monomer excluded volume. On the other hands, each bond cannot be longer than or equal 4(=√16) as Figure 1(d), which avoids a bond-crossing event.[27]

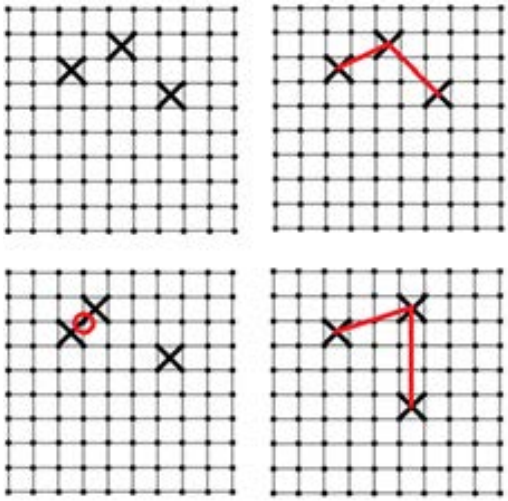

Figure 1. Some representative configurations of monomers and polymer chains in the BFM. (a) and (b) are typically allowed three monomers and a polymer chain and , (c) and (d) are forbidden structures.

To sample the trajectory, we randomly choose a monomer and try to move the chosen monomer to any direction by one lattice spacing. Validated with SAW condition, the new configuration is decided to accept or to reject. If we call a Monte Carlo sweep that the number of tries is the same with the number of monomers in a system.

Results and Discussions

A. Flory Exponent

Before explaning our results, I briefly explain a simple theory which deals with a SAW polymer considering monomer excluded volume often referred to Flory theory. In this theory, the free energy of a 2D polymer is written in terms of the polymer size *R* and degree of polymerization *N*. In dilute good solvent condition, entropic and enthalpic contributions compete each other, and the free energy is expressed by:[9]

$$F_{ent} \approx kT\frac{R^2}{Nb^2} \quad (1)$$

$$\frac{F_{int}}{V} = \frac{kT}{2}(vc^2 + wc^3 + \cdots) = kT\,(v\frac{N^2}{R^4} + w\frac{N^3}{R^6} + \cdots) \quad (2)$$

$$F_{int} \approx kT(v'\frac{N}{R^2}^2) \ (\text{Volume} \propto \text{R}^2) \quad (3)$$

$$0 = \frac{dF}{dR} \approx \frac{d}{dR}\left(kT\left(\frac{R^2}{Nb^2} + v'\frac{N}{R^2}^2\right)\right) = kT\left(\frac{2R}{Nb^2} - 2v'\frac{N}{R^3}^2\right) \quad (4)$$

$$\therefore R_F \approx v'^{1/4}b^{2/4}N^{3/4} \quad (5)$$

That is to say, there is a relationship that size of diluted polymer (It may means spanning distance -distance between one monomer and another opposite monomer- in the ring

polymer, while it means end-to-end distance in the linear polymer. For convenience's sake, we will call this spanning distance as end-to-end distance) in 2D is proportional to $N^{3/4}$. At this moment, we refer the exponent as power-law exponent or Flory exponent (ν). Since this Flory exponent equals to the inverse of fractal dimension (because the number of monomers or polymer's volume may proportional to $N^{1/\nu}$) it is important to identify (fractal) structure.

As we mentioned, diluted and not branched polymer in 2D has the Flory exponent, 3/4, however, solution becoming denser, a polymer may have different properties, it has ν =1/2, which coincides with the exponent of random-walking polymers in multi-dimension. It equals to the dimension of the plane where the polymer lay on since monomers are so crammed. If polymers almost approach fractal dimension of 2 and they are so crammed and interrupted, we call this phase as 'the melt phase'.[10,28]

Usually, 'maximal melt phase' which can confirm polymer movement at the well-pace is φ=0.8.[29] Thus this article reveals how structural properties are changed for change concentration from φ=0.016 to φ=0.8.

Here, we identify size parameter as degree of polymerization changes in dilute solution (φ=0.016) and the melt phase (φ=0.8). As a result, Flory exponent is nearly 0.75(3/4) in dilute solution while 0.5(1/2) in the melt phase. This means that polymers in dilute solution obey SAW statistics while polymers in the melt phase behave as monomers are crammed like we mentioned above. From now on, if there is no special mention, 'size' will mean polymer's or its sub-chains' 'degree of polymerization' (N-1) or 'the number of monomers' (N).

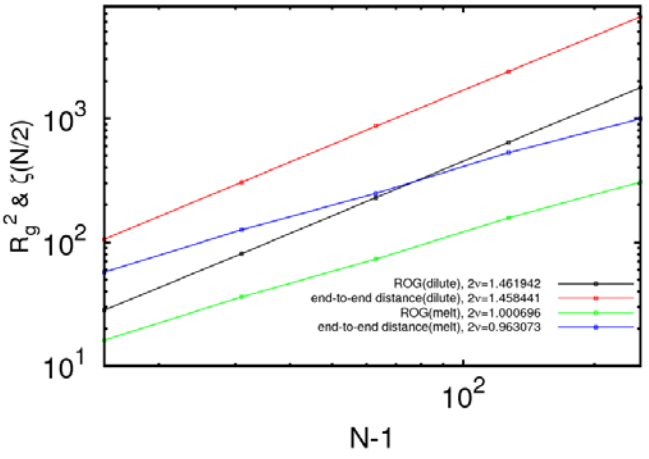

Figure 2. Log-log plots of gyration radii (black and green lines) and end-to-end distances (red and blue) as a function of degree of polymerization in dilute (φ=0.016) and concentrated regimes (φ=0.8). Slopes indicate 2ν.

Furthermore, referring to equation (6)[23], we plot end-to-end distance against size of sub-chains, and we more precisely obtain Flory exponent. According to this plotting results shown in Figure 3, we obtain ν=0.75 in dilute solution. However, we may obtain ν>0.5 (approximately, it is near 9/16) in the melt phase. This result means even in the same concentration, their exponents (and structural properties) are different to each other and each of them obeys different effects. In addition, the fact that in Figure 3 the shape of graphs maintains linearly until the subchain length reaches half of the whole chain length. This finding strongly supports that a ring is divided into two SAW linear sub-chains. Using these conclusions, we identify how to change detailed structures for the change of concentration using single molecule structure factors, etc.[6]

$$\zeta(s) = (const) \cdot \frac{s^{2\nu}(N-s)^{2\nu}}{s^{2\nu}+(N-s)^{2\nu}}\ , \qquad (6)$$

where N means the polymer length.

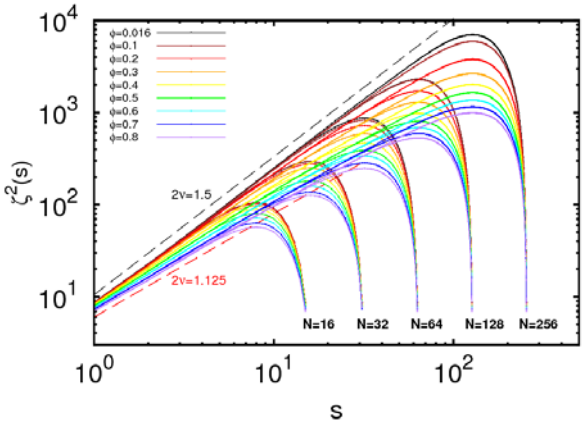

Figure 3. End-to-end distance as a function of sub-chain size on a log-log scale.

B. Single Molecule Structure Factor : $S(k)$

Now, we show single molecule structure factors of polymers. Structure factor is calculated using equations (7-9), and it means how many monomers within the length scale of 1/k is, where k means wavenumber in this function with dimension of inverse of lengths. In other words, when k is small (1/k is large), the structure factor has the number of monomers in a polymer. However, if k goes bigger (1/k will be smaller), structure factor will decay proportional to inverse of polymer's fractal dimension.[30]

$$S(k) = \frac{1}{N} < |\sum(e^{i\boldsymbol{k}\cdot\boldsymbol{r}})|^2 >_{|k|} \approx \frac{1}{N} < \sum_{i,j} \frac{\sin(kr_{ij})}{kr_{ij}} >_k \qquad (7)$$

$$S(k) \approx N(1 - \frac{1}{3}k^2) \ < R_g^2 > \rightarrow N \ \ (\mathrm{k{\cdot}Rg{<<}1}) \qquad (8)$$

$$S(k) \propto (kb)^{-D} \ \ (1/<R_g> << \mathrm{k} < 1/\mathrm{b}) \qquad (9)$$

Hence, Figure 4-7 show normalized single molecule structure factors.

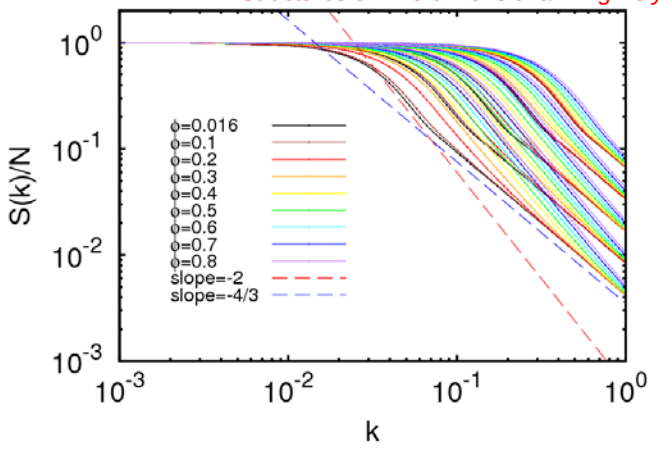

Figure 4. Structure factor in various *N*=16, 32, 64, 128, 256 and various density. Lines from left to right mean the polymer sizes of from big to small ones.

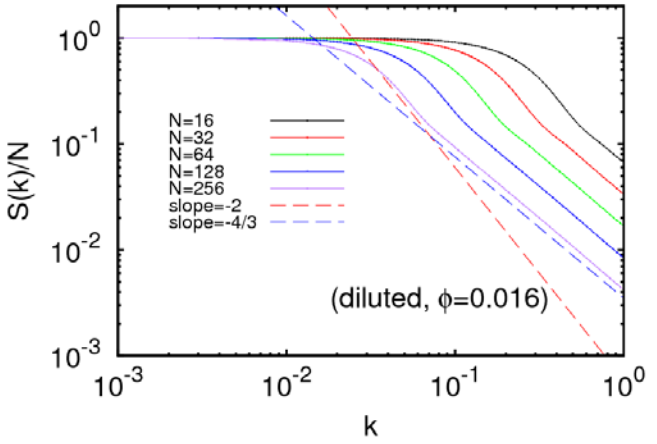

Figure 5. Structure factor in dilute solution (φ=0.016).

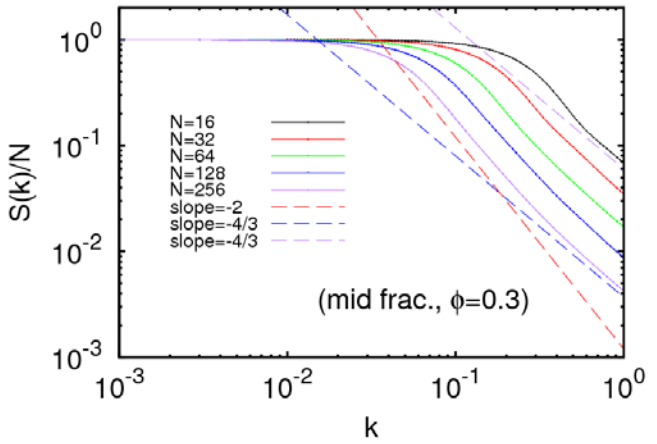

Figure 6. Structure factor in mid-concentration solution (φ=0.3).

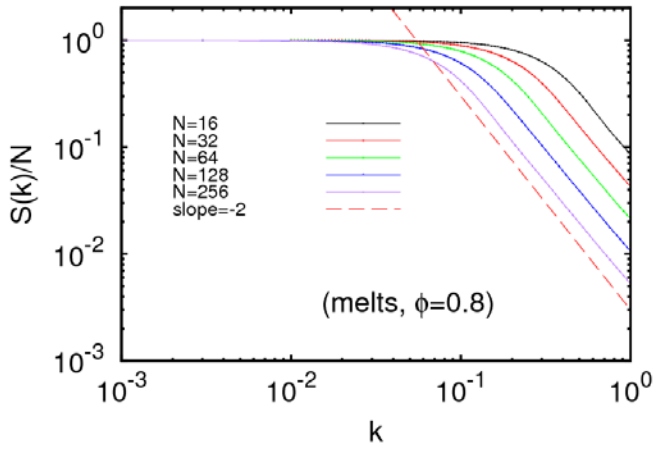

Figure 7. Structure factor in the melt phase (φ=0.8).

In above graphs, the bigger polymer, the more graph obviously moves left, since the larger polymer should occupy more space. Watching above Figure 4-7, you can catch that the structure factors decay differently as varying the concentration of polymer. At first, the thicker polymer, the more graph moves right because polymer collapse and become smaller. More to the point, decaying slope is -1.9~-2 in the small regime while it is -4/3 in a little larger regime in dilute solution. Because in the small regime, sub-chains obey SAW statistics, while the connected chain end of a ring induces that fractal dimension goes 2.

On the other hand, it seems that the decaying slope is -1.9~-2 in the wide regime in the melt phase because Flory exponent goes $\nu \approx 1/2$ in this phase. We will discuss about these phenomenon and directive statistics in more detail in a later section.

In addition, although polymers are in the same concentration (φ=0.3, medium concentration), when polymer size (*N*) is 16, polymers behave like dilute solution while when polymer size (*N*) is 256, the slope does not vary during decay with the value of -2 which reflects the melt phase. Thus, it also strongly suggests that in a certain concentration, rings of different degree of polymerization follow different statistics even though they have the same concentration. Therefore, we have to replot the structure factor considering polymer size (in this phrase, it means like radius of gyration) and concentration effect.

C. Bond Correlation Function

At this time, we calculate bond correlation functions (BCF) as a function of contour length in order to find regularities of bond vectors. Obtained results is plotted is Figure 8 and Figure 9.[31]

$$\mathbf{G}(|\mathbf{i}-\mathbf{j}|) = < \frac{|\vec{r_i} \cdot \vec{r_j}|}{|\vec{r_i}||\vec{r_j}|} >_{(i,j)} \qquad (13)$$

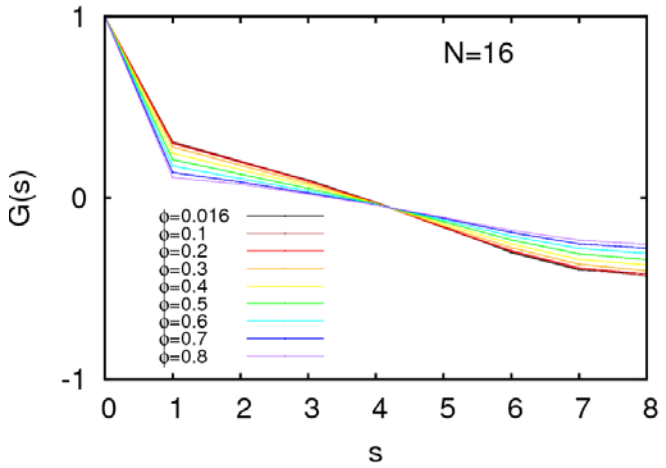

Figure 8. BCFs for small polymers (*N*=16) in different concentrations.

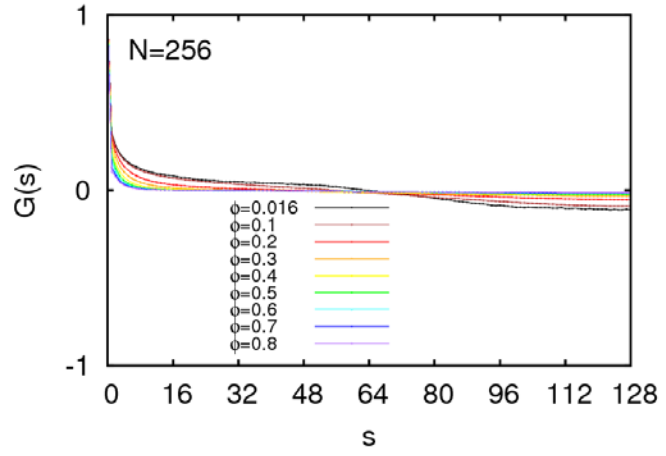

Figure 9. BCFs for large polymers (*N*=256) in different concentrations.

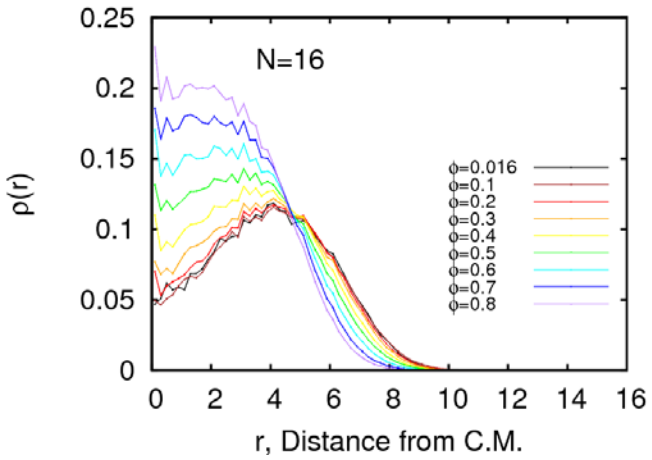

Figure 10. Density distribution functions from the polymer center of mass for a small polymer (*N*=16) in different concentrations.

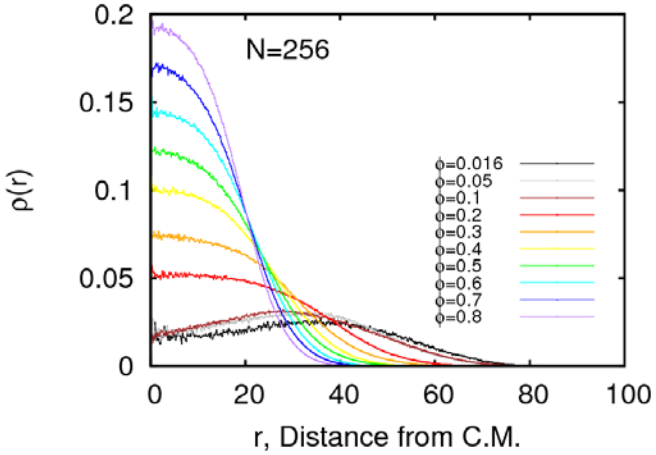

Figure 11. Density distribution functions from the polymer center of mass for larger polymer (*N*=256) in different concentrations.

Figure 8 and Figure 9 show that for dilute conditions, if two bond vectors are so far (the contour length is more far than *N*/4 and closer than *N*/2) there are a little anti-correlation because the polymer has almost circular shape. However, in the melt phase, the correlation rapidly disappears as the contour length increases, and no anti-correaltion is observed. This result infers the ring polymer is composed of a number of 'blobs' in which monomers obey SAW statistics individually.[32] In dilute concentration, this blob is very large and contains almost half of the whole monomers, but it becomes smaller with increasing the concentration.

D. Density Distribution Function from Center of Mass

We calculate monomer density distributions from the polymer center of mass which are normalized by the number of monomers to identify how monomers spread from center of the polymer.[33]

$$\int \boldsymbol{\rho}(\boldsymbol{r})\boldsymbol{d}\,\mathbf{r} = \boldsymbol{N} \qquad (11)$$

Figure 10 & 11 shows that monomers are densely populated around the radius of gyration (R_g) in dilute solution because of its pseudo-circular structure. However, as the concentration increases, monomers are focused on the center of polymer. In particular, very deep correlation hole is observed for N=256 ring polymer melts, thus it is very hard to find an evidence for interpenetration of other molecules into a ring. Therefore, according to BCFs and density distribution functions, we conclude that polymers in a melt have un-entangled and segregated structures because there are no regularity about bonding or structure and there are too few monomers far from the center.

In addition, as well as other structural properties, there are different concentration effect for different polymer sizes. When polymer is small, distribution in dilute solution is similar to distribution in relatively high concentration, however, when polymer is large, monomers are rapidly crumpled into the center of polymer for the change of concentration. Thus, we need to compare monomer distribution functions to find concentration effect precisely

which are plotted on the same 'normalized' concentration.

E. Overlap Concentration & Semidilute Solution

In previous sections, we described structures in dilute solution, the melt phase and intermediate states. Now, we define 'dilute solution concentration', boundary of two phase, dilute solution and the melt phase. To do so, we introduce the concept of overlap concentration. Overlap concentration means is the concentration at which the monomer concentration in a pervaded volume of a single polymer becomes the same with an average monomer concentration of the system. In very dilute regime, a pervaded volume divided by the number of monomers in a polymer is much large than an average volume occupied by a single monomer. Therefore, polymers does not overlapped to each other. However, in the concentrated regime, the system concentration is larger than the local concentration of a polymer, thus the polymers overlap. We can calculate the overlap concentration using the following equation. [34,35]

$$\varphi^* = \frac{N}{\pi R_g^2} \propto N^{-1/2} \quad (12)$$

First of all, we plot the contraction factor, $\mathbf{F(\varphi)} = \frac{R_g^2(\varphi)}{R_{g0}^2}$, where R_{g0} means radius of gyration in very dilute solution as a function of monomer concentration in Figure 12.

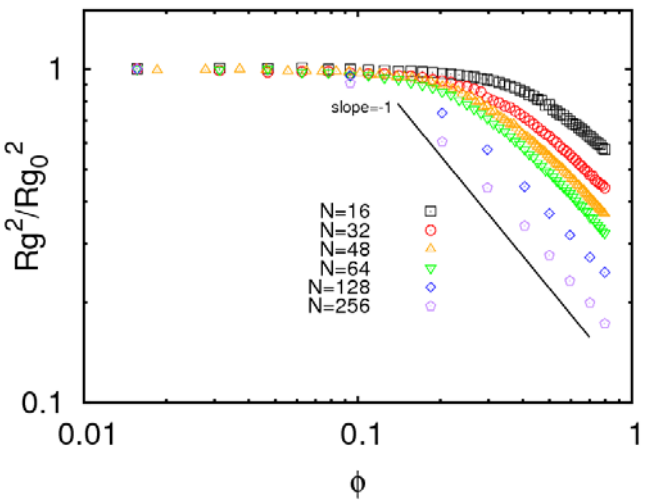

Figure 12. Contraction factor as a function of monomer concentration for rings of different degree of polymerization on a log-log scale.

According to Figure 12, at first glance, there seems no association among concentration, contraction factor, polymer size. However, it is noticeable to look at the decay rate as the density increases from 0.1 to 1.0. After we define over-lap concentration like $\boldsymbol{\varphi^* = N/\pi R_{g0}^2 \propto N^{-1/2}}$, you can see marvelous merging of all contraction factors in a single line regardless of density and degree of polymerization..

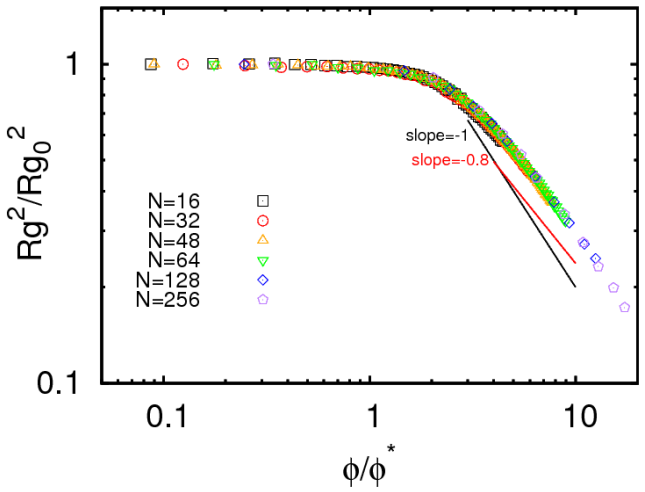

Figure 13. Contraction factor as a function of the ratio of concentration of polymer to overlap concentration on a log-log scale.

In addition, adding correction term($R_{g0}/2R_0$) to overlap con-centration which takes into account for the interpenetration as well as linear polymers written like (13), we try to plot a new graph based on equation (13).[34,35]

$$\boldsymbol{\varphi^{**} = \frac{N}{[2^{1/2}(R_{go}/a + R_{g0}/2R_0)]^2}} \quad (13)$$

In equation (13), R_0 means end-to-end distance and a means Kuhn's length. This model is athermal and the Kuhn length is also density-dependent, but for simplicity, we postulate a=1 which are the half of minimum of bond length. Unfortunately, those are less coherent than Figure 13, thus our definition of the overlap concentration is more reasonable for ring polymers, which considers a sphere-like shape of the ring.

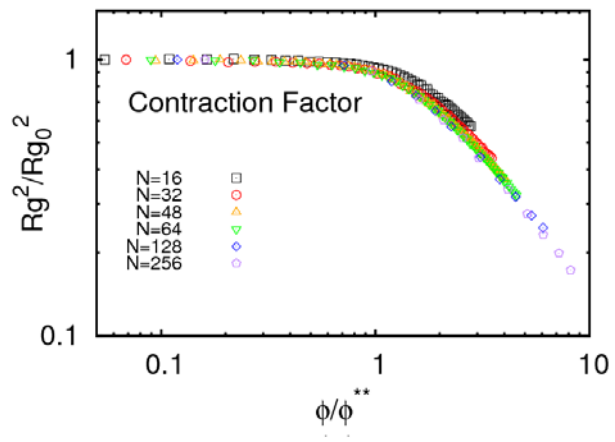

Figure 14. Contraction factor as a function of the ratio of concentration of polymer to overlap concentration which has one more correction term on a log-log scale.

In Figure 13, 'contraction' occurs at φ/φ^*=2~3 not at

$\varphi/\varphi^*\equiv1$, but is should be noted that the prefactor in calculating overlap concentration does not change the exponent of contraction factor but changes the absolute value of transition. It is expected that this prefactor is caused by the non-spherical shape of the ring, i.e., an ellipsoidal shape. Putting them together, overlap concentrations ($\boldsymbol{\varphi^* = N/\pi R_g^2}$) can be calculated as in Table 1.

Number of Monomers	Overlap Concentration
16	0.180
32	0.126
48	0.103
64	0.0890
128	0.0636
256	0.0460

Table 1. Overlap concentration vs. polymer size.

Now, applying this definition of overlap concentration, we can more easily describe various structural properties, because we now compare systems having the same normalized concentration (φ/φ^*).

First of all, we replot single molecule structure factors as a function of 'normalized wavevector' (kR_g) which means wavevector (k) multiplied by polymer's radius of gyration (R_g) like Figure 15 and 16 and try to compare among polymers which have the same normalized concentration (φ/φ^*).

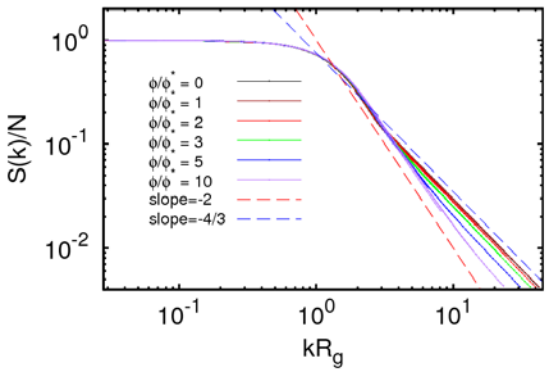

Figure 15. Structure factor normalized by polymer size in different normalized density. Graphs of various size (N=16, 32, 64, 128, 256) are overlapped.

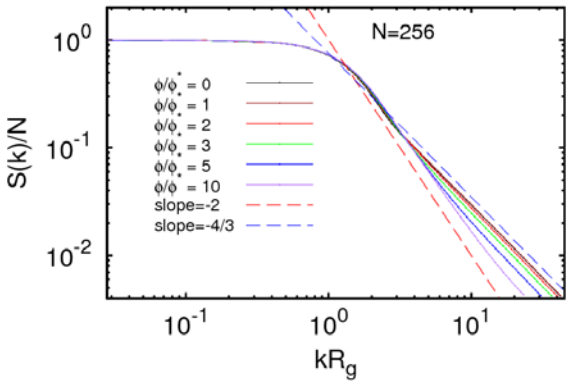

Figure 16. Structure factor (N=256, normalized).

According to Figure 15 and 16, polymers which have the same normalized concentration have almost same structure factor and show similar structural properties regardless of polymer length. Furthermore, comparing $S(k)$ at different concentration, they almost equally decay with the slope of -2 and are furcated at almost same spot. (kR_g=3) Finally, if normalized concentration are not too dense, nevertheless there are difference of pace of approaching, polymers follow SAW until the length scale of the wavevector decreases to the polymer size of the length $N/2$. In addition, difference of pace of approaching means that the range where sub-chains obey SAW statistics is different. Therefore, as mentioned above, SAW blobs become smaller with increasing the monomer density.

And, when we calculate BCF or density distribution function, looking at changing graph's shape for changing concentration, graph's shape are maintained at relatively high concentration, where the polymer are so small, however, graph's shape goes rapidly to melt phase's that where the polymer are so large.

Conclusion

To sum those all up, a 2D ring polymer simulated by BFM adopts pseudo-circular shape and obeys SAW statistics in dilute solution. However, beyond overlap concentration, they start to collapse and finally become the melt phase. However, they are not entangled with other polymers and segregated. In this context, we define the overlap concentration such that $\boldsymbol{\varphi^* = N/\pi R_g^2}$. Surprisingly, structural functions i.e. radius of gyrations, end-to-end distances, structure factors, bond correlation functions and density distribution functions can be describe only by relative concentration (φ/φ^*) regardless of polymer size.

Acknowledgments. This work has been supported by the project EDISON (EDucation-research Integration through Simulation On the Net), Chemistry and Seoul National University College of Natural Science Undergraduate Internship Program.

Reference

1. F. Drube, K. Alim, G. Witz, G. Dietler, E. Frey, *Nano Lett* **2010**, 10 (4), 1445–1449
2. T. Sakaue, G. Witz, G. Dietler, H. Wada, *EPL* **2010**, 91(6), 68002
3. B. Maier, J. O. Rädler, *Macromolecules*, **2001**, 34, 5723-5724
4. A. N. Semenov, J. Bonet-Avalos, A. Johner, J. F. Joanny, *Macromolecules* **1996**, 29(6), 2179-2196.
5. P. G. De Gennes, *Advances in Colloid and Interface Science* **1987**, 27(3-4), 189-209.
6. K. Kremer, G. S. Grest, *J. Chem. Phys* **1990**, 92(8), 5057-5086.
7. C. Tzoumanekas, D. N. Theodorou, *Macromolecules* **2006**, 39(13), 4592-4604.
8. G. Witz, K. Rechendorff, J. Adamcik, G. Dietler, *Phys. Rev. Lett* **2011**, 106, 248301
9. M. Rubistein, R. H. Colby, Polymer Physics, *Oxford University Press* **2003**, p. 102-103
10. P. G. De Gennes, Scaling Concepts in Polymer Physics, *Cornell University Press* **1979**, p. 54-55
11. I. Carmesin, K. Kremer, *J. Phys. France*, **1990** 51, 915-932
12. J. P. Wittmer, H. Meyer, A. Johner, T. Kreer, J. Baschnagel, *Phys. Rev. Lett.* **2010**, 105, 037802
13. M. E. Cates, J. M. Deutsch, *J. Physique* **1986**, 47, 2121
14. M. Bohn, D. W. Heermann, O. Lourenco, C. Cordeiro, *Macromolecules* **2010**, 43, 2564-2573
15. T. Sakaue, *Phys. Rev. Lett.* **2011**, 106(16), 167802
16. T. Sakaue, *Phys. Rev. Lett.* **2012**, 85(2), 021806
17. M. Kapnistos, M. Lang, D. Vlassopoulos, W. Pyckhout-Hintzen, D. Richter, D. Cho, T. Chang, M. Rubinstein, *Nat. Mater.* **2008**, 7(12), 997-1002
18. Z. C. Yan, S. Costanzo, Y. Jeong, T. Chang. D. Vlassopoulos, *Macromolecules* **2016**, 49(4), 1444
19. E. Lee, S. Kim, Y. Jung, *Macromol. Rapid Commun.* **2014**, 36(11), 1115-1121
20. E. Lee, Y. Jung. *Soft Matter*, **2015**, 11, 6018-6028
21. J. D. Halverson, W. B. Lee, G. S. Grest, A. Y. Grosberg, K. Kremer, *J. Chem. Phys.* **2011**, 134, 204904
22. A. Rosa, R. Everaers, *Phys. Rev. Lett* **2014**, 112, 118302
23. G. Witz, K. Rechendorff, J. Adamcik, G. Dietler, *Phys. Rev. Lett* **2008**, 101, 148103
24. M. Bishop, J. P. J. Michels, *J. Chem. Phys.* **1985**, 83, 4791
25. M. Bishop, J. P. J. Michels, *J. Chem. Phys.* **1986**, 85, 1074
26. Y. Oh, H. W. Cho, J. Kim. C. H. Park, B. J. Sung, *Bull. Korea Chem. Soc*, **2012**, 33(3), 975-979
27. I. Carmesin, K. Kremer, *Macromolecules* **1988**, 21(9), 2819-2823
28. J. Klein, *Nature* **1978**, 271, 143-145
29. H. Wittmann, K. Kremer, K. Binder, *J. Chem. Phys* **1992**, 96(8), 6291-6306
30. Rubistein, Colby, *op. cit.*, p. 82-88
31. A. Baumgärtner, *J. Chem. Phys* **1982**, 76(8), 4275-4280.
32. P. De Gennes, *Macromolecules* **1980**, 13(5), 1069-1075.
33. J. Wilhelm, E. Frey, *Phys. Rev. Lett* **1996**, 77(12), 2581
34. A. Yethiraj, *Macromolecules* **2003**, 36(15), 5854-5862.
35. I. Teraoka, Y. Wang, *Macromolecules* **2000**, 33(18), 6901-6903.